

Supporting Information for “Heterogeneous high frequency seismic radiation from complex, multi-phase ruptures”

Sara Beth L. Cebry¹, Gregory C. McLaskey¹

¹Cornell University, New York, USA

Contents of this file

1. Figures S1 to S7

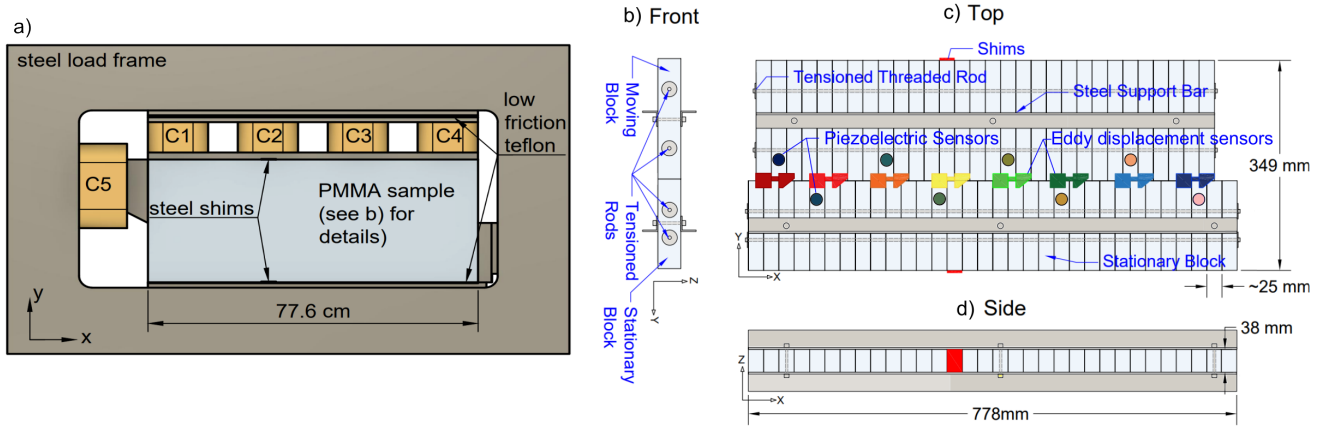


Figure S1. Schematic of biaxial loading frame (a) and details of the PMMA composite sample (b) showing how the sub-blocks were oriented and connected. (b-d) also shows the locations of piezoelectric ground motion sensors and eddy displacement sensors.

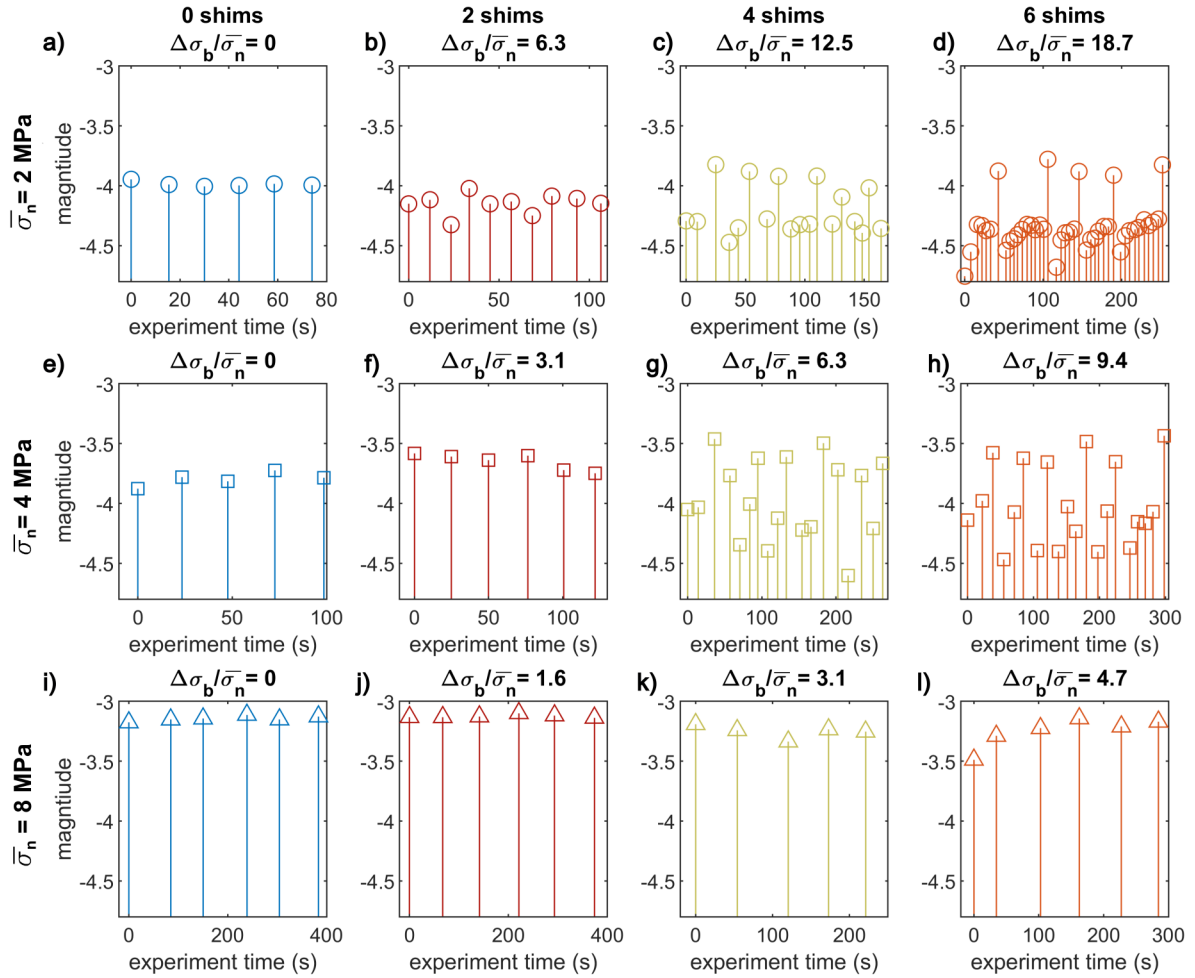


Figure S2. Moment for each event from all experiments in this study. Rows are conducted at the same $\bar{\sigma}_n$, with circles to represent experiments at 2 MPa, squares at 4 MPa, and triangles at 8 MPa. All columns are conducted with the same number of shims (0, 2, 4, and 6 shims) as indicated by color. This produced results over a range of bump prominence from 0 to 18.7. Subplots share the same y-axis scale, but the x-axis varies by experiment for clarity.

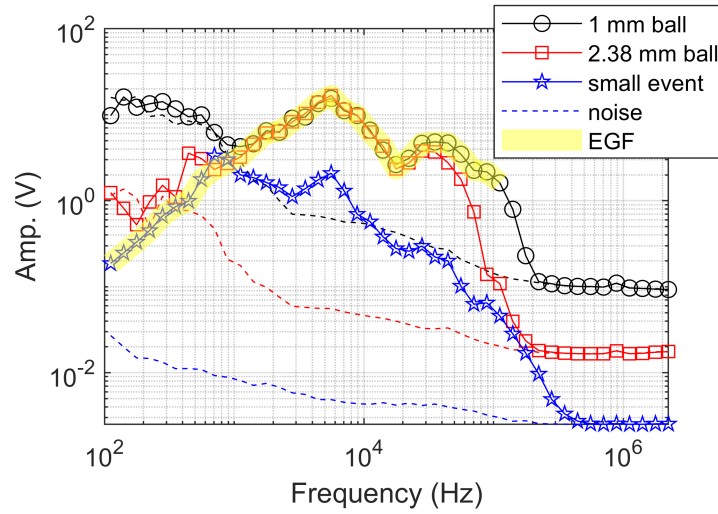


Figure S3. Spectra of 1 mm ball drop, 2.38 mm ball drop, and small event concatenated to create the empirical green’s function that is used to calculate the true source spectra. Ball spectra are scaled by equivalent moment calculated with from the change in momentum when the ball hit the sample. The small event spectra is scaled so it matches with the 2.38 mm ball around 1 kHz. Noise spectra are computed from a noise window the same size as the spectra taken after the ball drops were finished.

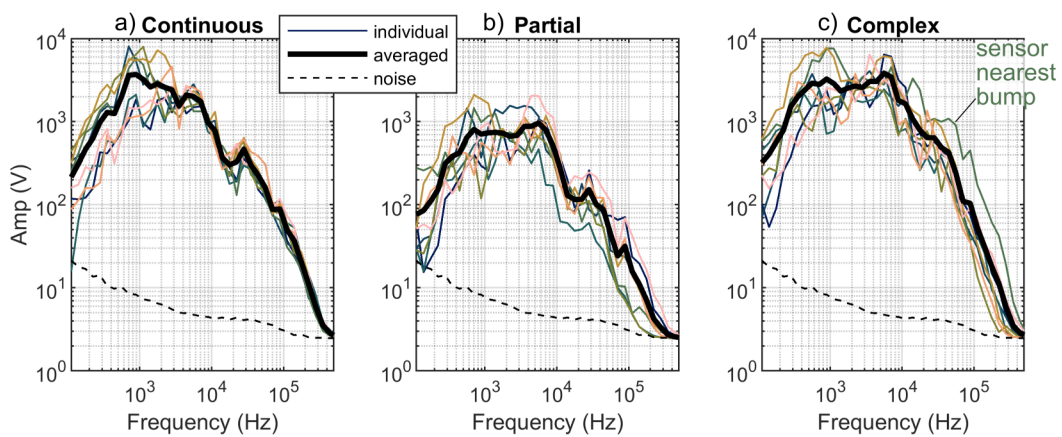


Figure S4. Uncorrected spectra for individual sensors plotted for the three representative events. Sensors are color-coded to match Figure S1 with dark blue at $x = 0$ m and light pink at $x = 0.74$ m. The average of all spectra is shown in the bold black line. The noise level is shown with a dashed line.

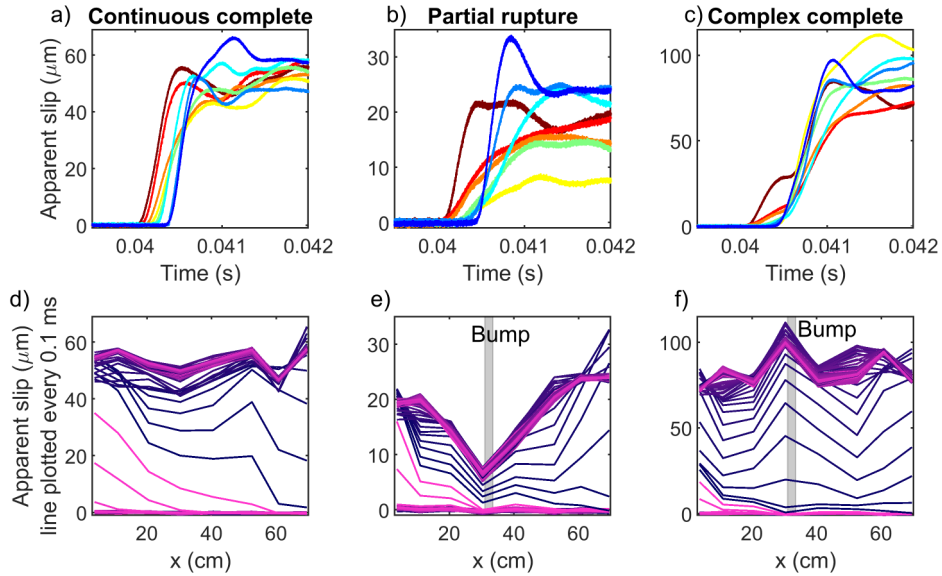


Figure S5. Apparent slip measurements for three events. a-c) apparent slip as a function of time. Sensors are color-coded to match Figure S1 with red at $x = 0$ m and dark blue at $x = 0.74$ m. d-f) show the same data but as a function of space and time for a 0.08 s window centered around the event. Each line represents the apparent slip along the fault at a snapshot in time. Lines are plotted every 0.05 ms. Colors cycle from light pink to dark purple every 2.5 ms.

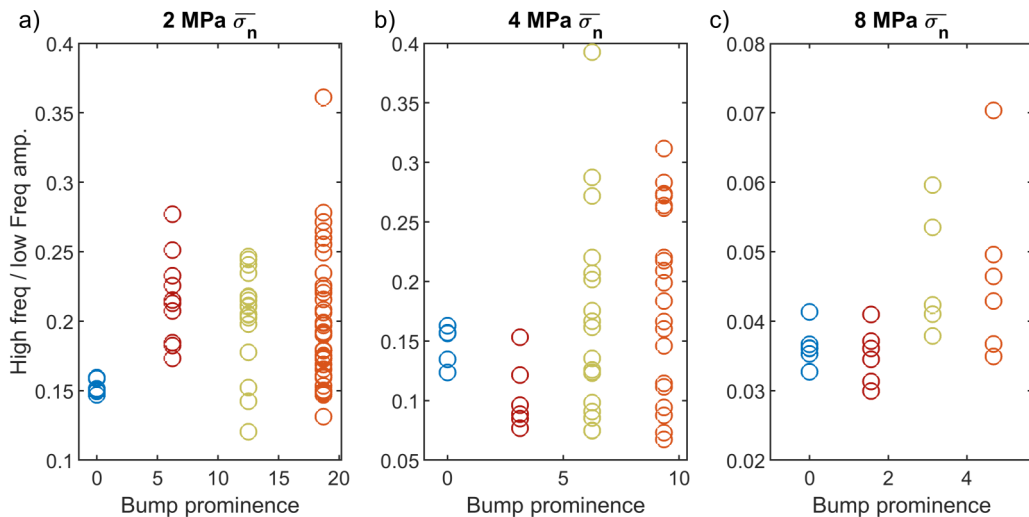


Figure S6. Spectra amplitude between 2.8 and 4 kHz (high frequency) divided by spectra amplitude between 100 and 180 Hz (low frequency) for each event from a total of 12 different experiments at 2, 4, and 8 MPa $\bar{\sigma}_n$, each with four bump prominence levels.

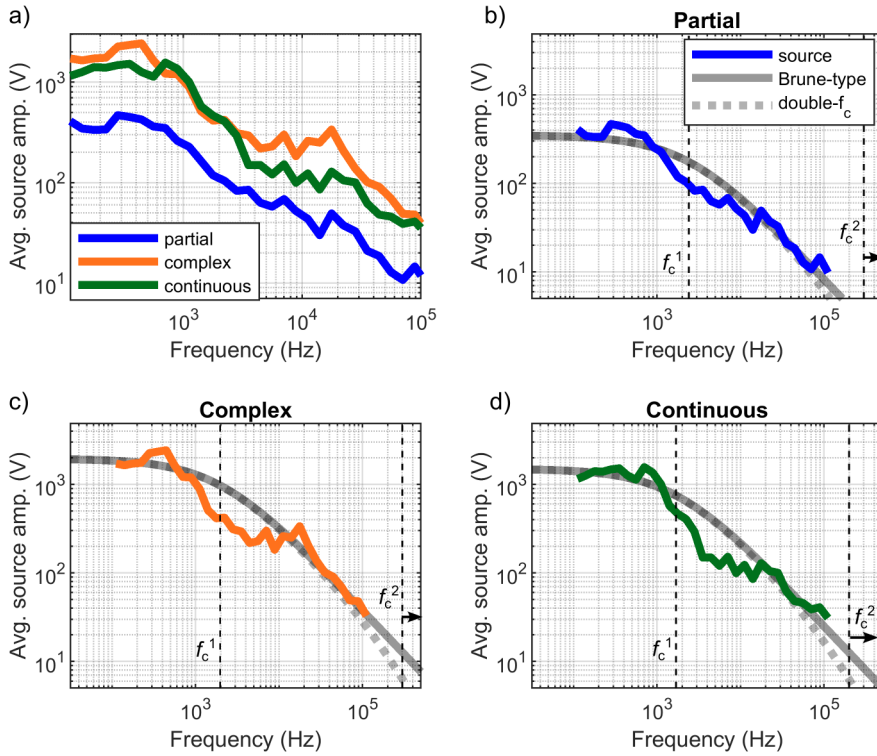


Figure S7. Source spectra (solid, colored lines) compared to Brune-type source model (solid grey lines) and a double-corner frequency model (dashed, thick grey lines) for the three representative events. f_c^1 is marked with a thin, black dashed line. f_c^2 cannot be identified with the frequency range for our source spectra, however a lower bound for f_c^2 is shown with a thin, black dashed line.

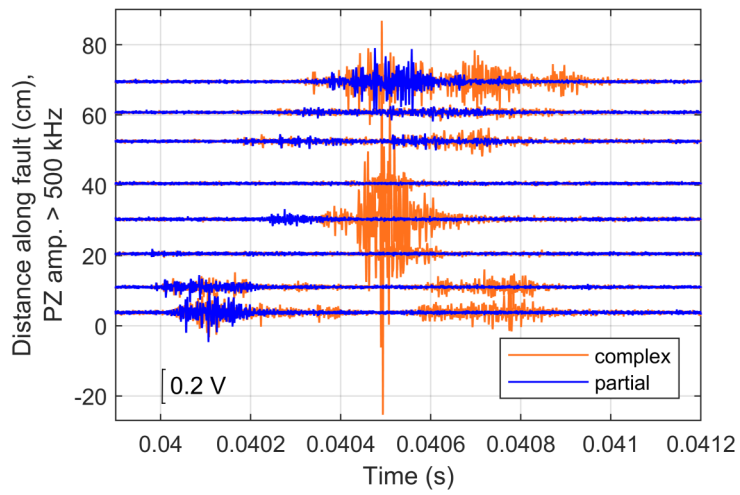


Figure S8. High frequency (greater than 500 kHz) ground motions for a complex (orange) and a partial (blue) rupture overlaid for comparison. Measurements are offset by sensor location along the fault.